Constrained Nonlinear Tracking Control for Small Fixed-wing Unmanned Air Vehicles

Wei Ren Randal W. Beard*
Department of Electrical and Computer Engineering
Brigham Young University
Provo, Utah 84602
{weiren,beard}@ee.byu.edu

***Abstract*— This paper considers the problem of constrained nonlinear tracking control for small fixed-wing unmanned air vehicles equipped with longitudinal and lateral autopilots. Four different controllers based on SDRE, Sontag's formula, geometric parameterization, and saturation are proposed and compared to show their strength and weakness under different application scenarios. Issues of measurement noise and input uncertainties are also addressed under the input-to-state stability framework. The effectiveness of the approaches are demonstrated through detailed simulation studies.**

I. Introduction

Controller design for systems subject to input constraints offers both practical significance and theoretical challenges to the control community. Although significant progress has been made for constrained linear systems (see [1], [2]), much fewer results are available for constrained nonlinear systems, especially those systems with nonholonomic constraints.

Two effective approaches for the design of nonlinear controllers are control Lyapunov functions (CLFs) [3], [4] and receding horizon control (RHC), also named as model predictive control (MPC), [5], [6], [7]. Both approaches can be extended to find control laws for nonlinear systems subject to certain input constraints. In [8] and [9], constrained CLFs are applied to construct stabilizing universal formulas respectively for systems with control inputs bounded in a 2-norm sense and systems with a scalar control input that is positive and/or bounded. Input constraints can also be incorporated into the MPC framework, which is known as the constrained MPC (c.f. [6]). The issues existing in the RHC approach are its computation intensity and stability concerns, which motivates the technique involving a combination of the CLF approach and RHC approach [10], [11].

In this paper, we consider the problem of constrained nonlinear tracking control for small fixed-wing unmanned air vehicles (UAVs). The inherent properties of the fixed-wing UAVs impose the input constraints of positive miminum velocity, bounded maximum velocity, and saturated heading rate. Equipping the UAVs with standard longitudinal and lateral autopilots, their dynamics can be modeled by kinematic equations of motion that are similar to those of nonholonomic mobile robots. However, the saturated tracking control laws for mobile robots [12], [13] are not directly applicable to our problem since negative velocities are allowed in their approaches.

*Corresponding author.

In [14], a constrained tracking CLF is constructed and a simple saturation controller based on this CLF is proposed for the UAV tracking control problem, where issues like input uncertainties and measurement noise are not considered. In this paper, we extend the results in [14]. We propose four different tracking controllers and compare them with each other to show relative strength and weakness under different situations. Among them, the first one is based on the state dependent Riccati equation (SDRE) approach [15], [16], the second one is based on Sontag's formula, the third one is based on a geometric approach, and the last one follows the saturation controller in [14] but explicitly accounts for input uncertainties under the input-to-state (ISS) framework [17]. Although our approach is designed specifically for certain system dynamics, the design strategy can be applied to general systems. That is, if a constrained CLF can be found for a system with input constraints, the feasible set that defines all the stabilizing controls with respect to the CLF satisfying the input constraints can be specified accordingly (see [18] for a complete parameterization of the unconstrained stabilizing controls with respect to a certain CLF). Then any existing approach that may not account for input constraints such as universal formulas, min-norm formulas, backstepping, sliding mode, SDRE, LQR, and so on can be projected to the feasible set in a certain way. Different projection strategies can be chosen based on different applications, for example, find the closest elememt in the set. The resulting control law not only guarantees stability but also satisfies input constraints. In addition, direct parameterization of the feasible set, for example, geometric approach, can also be applied. Of course, the above design methodology requires finding a constrained CLF, which may be challenging for general nonlinear systems.

The remainder of the paper is organized as follows. In Section II, we state the UAV control system architecture and the constrained tracking control problem. In Section III, we propose nonlinear tracking controllers based on the SDRE approach and Sontag's formula. In Section IV, a constrained tracking controller based on a geometric approach is presented and input uncertainties are considered for a saturation controller. Section V offers detailed simulation results for these four controller and Section VI contains our conclusion.

II. Problem Statement

The overall system architecture considered in this paper consists of five layers [19]: Waypoint Path Planner (WPP), Dynamic Trajectory Smoother (DTS), Trajectory Tracker (TT), Longitudinal and Lateral Autopilots, and the UAV as shown in Figure 1.

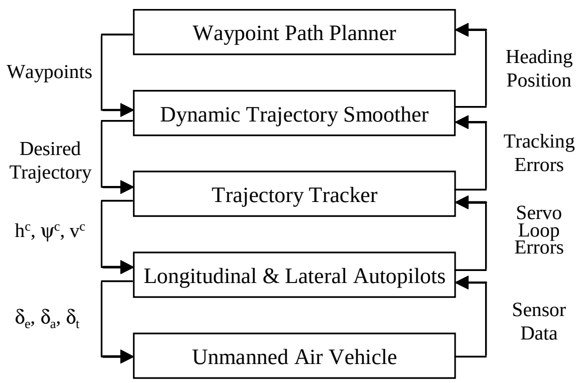

Fig. 1. System Architecture.

The WPP generates waypoint paths (straight-line segments) that change in accordance with the dynamic environment consisting of the location of the UAV, the targets, and the dynamically changing threats. The DTS smoothes through these waypoints and produces a feasible time-parameterized desired trajectory, that is, the desired position $(x_r(t), y_r(t))$, heading $\psi_r(t)$, and altitude $h_r(t)$. The TT outputs the desired velocity command v^c, heading command ω^c, and altitude command h^c to the autopilots based on the desired trajectory. The autopilots then use these commands to control the elevator, δ_e, aileron, δ_a, deflections and the throttle setting δ_t of the UAV.

With the UAV equipped with standard autopilots [20], the resulting UAV/autopilot models are assumed to be first order for heading and Mach hold, and second order for altitude hold [21]. Letting (x, y), ψ, v, and h denote the inertial position, heading angle, velocity, and altitude of the UAV respectively, the kinematic equations of motion are given by

$$\begin{aligned}
\dot{x} &= v\cos(\psi) \\
\dot{y} &= v\sin(\psi) \\
\dot{\psi} &= \alpha_\psi(\psi^c - \psi) \\
\dot{v} &= \alpha_v(v^c - v), \\
\ddot{h} &= -\alpha_{\dot{h}}\dot{h} + \alpha_h(h^c - h),
\end{aligned} \tag{1}$$

where ψ^c, v^c, and h^c are the commanded heading angle, velocity, and altitude to the autopilots, and α_* are positive constants [20].

Following [21], let the altitude controller be given by

$$h^c = h + \frac{1}{\alpha_h}[\ddot{h}_r + \alpha_{\dot{h}}\dot{h} - k_{\dot{h}}(\dot{h} - \dot{h}_r) - k_h(h - h_r)],$$

where h_r is the desired altitude, and k_h and $k_{\dot{h}}$ are positive constants.

Next we will focus on the design of the velocity and heading controller. We assume that the velocity-heading dynamics are adequately modeled by

$$\begin{aligned}
\dot{x} &= v^c\cos(\psi) \\
\dot{y} &= v^c\sin(\psi) \\
\dot{\psi} &= \omega^c,
\end{aligned} \tag{2}$$

where $\omega^c = \alpha_\psi(\psi^c - \psi)$ [14]. The dynamics of the UAV impose the following input constraints

$$\begin{aligned}
\mathcal{U}_1 = \{v^c, \omega^c | 0 < v_{min} \le v^c \le v_{max}, \\
-\omega_{max} \le \omega^c \le \omega_{max}\}.
\end{aligned} \tag{3}$$

The desired trajectory $(x_r, y_r, \psi_r, v_r, \omega_r)$ generated by the trajectory generator also satisfies Eq. (2) under the constraints that v_r and ω_r are piecewise continuous and satisfy the constraints

$$\begin{aligned}
v_{min} + \epsilon_v \le & v_r \le v_{max} - \epsilon_v \\
-\omega_{max} + \epsilon_\omega \le & \omega_r \le \omega_{max} - \epsilon_\omega,
\end{aligned} \tag{4}$$

where ϵ_v and ϵ_ω are positive control parameters.

By transforming the tracking errors expressed in the inertial frame as $(x_r - x, y_r - y, \psi_r - \psi)$ into the UVA body frame denoted as (x_e, y_e, ψ_e) and introducing variable changes [13], we obtain

$$\begin{aligned}
\dot{x}_0 &= u_0 \\
\dot{x}_1 &= (\omega_r - u_0)x_2 + v_r\sin(x_0) \\
\dot{x}_2 &= -(\omega_r - u_0)x_1 + u_1,
\end{aligned} \tag{5}$$

where

$$(x_0, x_1, x_2) = (\psi_e, y_e, -x_e) \tag{6}$$

and $u_0 \triangleq \omega_r - \omega^c$ and $u_1 \triangleq v^c - v_r\cos(x_0)$.

The input constraints under the transformation become

$$\mathcal{U}_2 = \{u_0, u_1 | \underline{\omega} \le u_0 \le \bar{\omega}, \underline{v} \le u_1 \le \bar{v}\}, \tag{7}$$

where $\underline{v} \triangleq v_{min} - v_r\cos(x_0)$, $\bar{v} \triangleq v_{max} - v_r\cos(x_0)$, $\underline{\omega} \triangleq \omega_r - \omega_{max}$, and $\bar{\omega} \triangleq \omega_r + \omega_{max}$.

Note from Eq. (5) that x_1 is not directly controlled by u_0 and u_1. To avoid this situation we introduce another change of variables.

Let $\bar{x}_0 \triangleq mx_0 + \frac{x_1}{\pi_1}$, where $m > 0$ and $\pi_1 \triangleq \sqrt{x_1^2 + x_2^2 + 1}$. Accordingly, $x_0 \triangleq \frac{\bar{x}_0}{m} - \frac{x_1}{m\pi_1}$. Obviously, $(\bar{x}_0, x_1, x_2) = (0, 0, 0)$ is equivalent to $(x_0, x_1, x_2) = (0, 0, 0)$ and $(x_e, y_e, \psi_e) = (0, 0, 0)$. The original tracking control objective, that is, find v^c and ω^c such that $|x_r - x| + |y_r - y| + |\psi_r - \psi| \to 0$ as $t \to \infty$, is converted to a stabilization objective, that is, find control inputs u_0 and u_1

to stabilize (x_0, x_1, x_2) or $(\bar{x}_0, x_1, x_2)$. With the same input constraints (7), Eq. (5) can be rewritten as

$$\begin{aligned}
\dot{\bar{x}}_0 &= (m - \frac{x_2}{\pi_1})u_0 + \frac{x_2}{\pi_1}\omega_r \\
&\quad + \frac{1+x_2^2}{\pi_1^3} v_r \sin\left(\frac{\bar{x}_0}{m} - \frac{x_1}{m\pi_1}\right) - \frac{x_1 x_2}{\pi_1^3} u_1 \\
\dot{x}_1 &= (\omega_r - u_0)x_2 + v_r \sin\left(\frac{\bar{x}_0}{m} - \frac{x_1}{m\pi_1}\right) \qquad (8) \\
\dot{x}_2 &= -(\omega_r - u_0)x_1 + u_1.
\end{aligned}$$

Define

$$W(x) = \gamma_0 \left(\frac{\bar{x}_0}{\pi_2}\right)^2 + \gamma_1 k_1 (v_{\min} + \epsilon_v) \frac{x_1}{\pi_1} \sin\left(\frac{x_1}{m\pi_1}\right)$$
$$+\gamma_2 \left(k_1 - \frac{1}{2}\right)\left(\frac{x_2}{\pi_1}\right)^2 \left((v_{\min} + \epsilon_v)\cos\left(\frac{x_1}{m\pi_1}\right) - v_{\min}\right), \qquad (9)$$

where $\pi_2 \triangleq \sqrt{\bar{x}_0^2 + 1}$, $k_1 > \frac{1}{2}$, $\gamma_0 > 0$, $0 < \gamma_1 < 1$, and $0 < \gamma_2 < 1$.

It has been shown in [14] that for $m > \kappa$, where κ is a positive constant made precise in [14],

$$V(x) = \sqrt{\bar{x}_0^2 + 1} + k_1 \sqrt{x_1^2 + x_2^2 + 1} - (1 + k_1) \qquad (10)$$

is a constrained CLF for system (8) with input constraints (7) such that

$$\inf_{u \in \mathcal{U}_2} \dot{V} \leq -W(x),$$

where $W(x)$ is a continuous positive-definite function given by Eq. (9).

III. Nonlinear Tracking Control for UAVs

In this section, we propose two nonlinear tracking controllers for UAVs. They have the property that input constraints are not explicitly considered. One controller follows the SDRE approach and the other is based on Sontag's formula.

A. SDRE Tracking Controller

The SDRE nonlinear regulator is derived to minimize the performance index

$$J = \frac{1}{2} \int_0^\infty x^T Q(x) x + u^T R(x) u dt$$

for the affine nonlinear system

$$\dot{x} = f(x) + g(x)u, \qquad (11)$$

where $x \in I\!R^n$, $u \in I\!R^m$, $Q(x) > 0$, $R(x) > 0$, $\forall x$, $f(x) \in C^1$, and $f(0) = 0$.

Motivated by the LQR approach (c.f. [22]) for LTI systems, Eq. (11) can be represented as

$$\dot{x} = A(x)x + B(x)u, \qquad (12)$$

where $A(x)x = f(x)$ and $B(x) = g(x)$.

Under the condition that the pair $(A(x), B(x))$ is pointwise stabilizable, the nonlinear state feedback control law can be constructed as

$$u_{SDRE} = -R^{-1}(x) B^T(x) P(x) x, \qquad (13)$$

where $P(x) > 0$ is obtained by solving the state-dependent Riccati equation

$$A^T P + PA - PBR^{-1}B^T P + Q = 0$$

pointwise at each state x.

It has been shown that the SDRE regulator is locally asymptotically stable and suboptimal [16].

To this end, system (5) can be rewritten as

$$\dot{x} = A(t,x)x + B(x)u,$$

where $x = [x_0, x_1, x_2]^T$, $u = [u_0, u_1]^T$,

$$A(t,x) = \begin{bmatrix} 0 & 0 & 0 \\ v_r(t)\frac{\sin(x_0)}{x_0} & 0 & \omega_r(t) \\ 0 & -\omega_r(t) & 0 \end{bmatrix}$$

and

$$B(x) = \begin{bmatrix} 1 & 0 \\ -x_2 & 0 \\ x_1 & 1 \end{bmatrix}.$$

The pointwise controllability matrix is given by $C(t,x) = [B(x), A(t,x)B(x), A(t,x)^2 B(x)]$. It can be verified that $C(t,x)$ has full rank when $\omega_r(t) \neq 0$. When $\omega_r(t) = 0$ at some time $t = t^*$, it can be seen that $C(t,x)$ still has full rank if and only if $x_0 \neq k\pi$, $k \in \mathbf{Z} \setminus 0$. As a result, $(A(t,x), B(x))$ is pointwise stabilizable as long as $x_0 \neq k\pi$, $k \in \mathbf{Z} \setminus 0$.

Note that unlike the standard SDRE regulation problem, matrix $A(t,x)$ factorized from Eq. (11) is also an explicit function of time since the reference velocity $v_r(t)$ and referece heading rate $\omega_r(t)$ are time-varying. The SDRE tracking controller will be obtained by following Eq. (13) except that the pointwise solution to the SDRE, denoted as $P(t,x)$, is also an explicit function of time in this case. This results from the fact that the state is regulated to a time-varying trajectory instead of a constant reference state. Also note that the SDRE controller is designed according to the original system (5) rather than the system (8) with variable changes, which may be superior to the controllers designed according to system (8) under some situations.

Define a saturation function as

$$\mathrm{sat}(\alpha, \beta, \gamma) = \begin{cases} \beta, & \alpha < \beta \\ \alpha, & \beta \leq \alpha \leq \gamma \\ \gamma, & \alpha > \gamma \end{cases}.$$

Note that the control $u_{SDRE} = [u_a, u_b]^T$ may not satisfy the input constraints (7). The actual control will be saturated to satisfy (7) according to a simple projection as follows:

$$\begin{aligned} u_0 &= \mathrm{sat}(u_a, \underline{\omega}, \bar{\omega}) \\ u_1 &= \mathrm{sat}(u_b, \underline{v}, \bar{v}). \end{aligned} \qquad (14)$$

B. Tracking Controller Based on Sontag's Formula

For system (11), a globally asymptotically stabilizing control law known as Sontag's formula [23], [24] is given by

$$u_s = \begin{cases} -\frac{L_fV+\sqrt{(L_fV)^2+(L_gV(L_gV)^T)^2}}{L_gV(L_gV)^T}(L_gV)^T, & L_gV \neq 0 \\ 0, & L_gV = 0 \end{cases} \tag{15}$$

where $V(x)$ is a CLF for system (11).

Note that Eq. (8) can be rewritten as

$$\dot{x} = f_1(t,x) + g_1(t,x)u, \tag{16}$$

where

$$f_1(t,x) = \begin{bmatrix} \frac{x_2}{\pi_1}\omega_r + \frac{1+x_2^2}{\pi_1^3}v_r \sin\left(\frac{\bar{x}_0}{m} - \frac{x_1}{m\pi_1}\right) \\ -x_2\omega_r + v_r \sin\left(\frac{\bar{x}_0}{m} - \frac{x_1}{m\pi_1}\right) \\ -\omega_r x_1 \end{bmatrix}$$

and

$$g_1(t,x) = \begin{bmatrix} m - \frac{x_2}{\pi_1} & -\frac{x_1x_2}{\pi_1^3} \\ -x_2 & 0 \\ x_1 & 1 \end{bmatrix}.$$

The tracking controller for UAVs based on Sontag's formula can be defined following Eq. (15) with $L_fV = \frac{\partial V}{\partial x}f(t,x)$ and $L_gV = \frac{\partial V}{\partial x}g(t,x)$, where $V(x)$ is the constrained CLF given by (10). Note that although the universal formula (15) is originally proposed for time-invariant systems, the formula is also valid for the time-varying system (16) due to the fact that the CLF for system (8) is not an explicit function of time. However, there is no guarantee that the control $u_s(t,x)$ given by Eq. (15) will satisfy the input constraints (7) since Sontag's formula is based on the assumption $u \in I\!R^m$. Similar to the SDRE controller, the actual control is a projection of $u_s(t,x) = [u_c, u_d]$ to the space defined by the input constraints (7) as follows

$$\begin{aligned} u_0 &= \mathrm{sat}(u_c, \underline{\omega}, \bar{\omega}) \\ u_1 &= \mathrm{sat}(u_d, \underline{v}, \bar{v}). \end{aligned} \tag{17}$$

IV. Constrained Nonlinear Tracking Control for UAVs

In this section, we present two other nonlinear tracking controllers which are designed explicitly accounting for input constraints.

A. Tracking Controller Based on Geometric Approach

Define the feasible control set as

$$\mathcal{F}(t,x) = \{u \in \mathcal{U}_2 | L_{f_1}V + L_{g_1}Vu \leq -W(x)\},$$

where $W(x)$ is given by Eq. (9). Note that the fact that V is a constrained CLF for system (16) guarantees $\mathcal{F}(t,x)$ is nonempty for any t and x.

Fig. 2 and 3 show the feasible set at time $t = t_1$ and $t = t_2$ respectively. The line denoted by $L_{g_1}Vu + L_{f_1}V + W = 0$

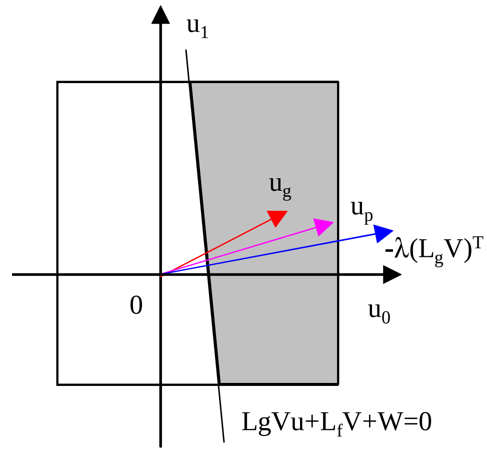

Fig. 2. The feasible set $\mathcal{F}(t,x)$ at time $t = t_1$.

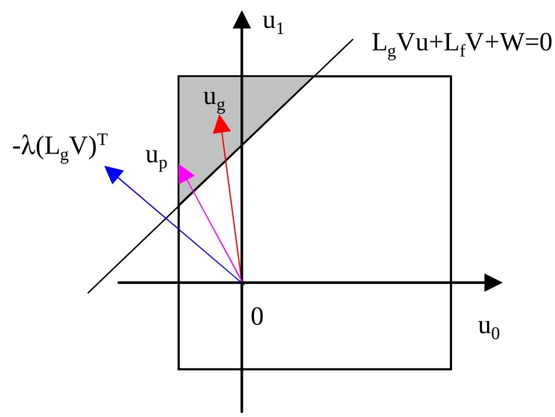

Fig. 3. The feasible set $\mathcal{F}(t,x)$ at time $t = t_2$.

separates the 2-D control space into two halves, where the right half in Fig. 2 and the left half in Fig. 3 represent the unconstrained stabilizing controls satisfying $\dot{V} \leq -W(x)$. The rectangle area denotes the input constraints (7), which is time-varying. The shaded area represents the stabilizing controls which also satify input constraints (7), that is, the feasible set $\mathcal{F}(t,x)$. In Fig. 2 and 3, u_g represents the control based on the geometric approach. Here we choose the geometric control u_g as the geometric center of the feasible set. Obviously, such controls will stay in the feasible set at each time.

As a comparison, we also plot the vector $-\lambda(L_{g_1}V)^T$ in both figures, where $\lambda > 0$. Note that this vector is orthogonal to the line $L_{g_1}Vu + L_{f_1}V + W = 0$. It can be verified that the control based on Sontag's formula in Section III-B can be represented as $u_s(t,x) = -\chi(t,x)(L_{g_1}V)^T$, where $\chi(t,x)$ is a nonnegative scalar function of t and x. Therefore, the control based on Sontag's formula lies along the vector $-\lambda(L_{g_1}V)^T$ but may have a different magnitude. In Fig. 2, we can see that the control based on Sontag's formula may or may not stay in the feasbile set depending on its magnitude. However, a proper scale of the control can always bring it back to the feasible set. With the input constraints (7), the actual control will be a projecton of $u_s(t,x)$ to the rectangle region. As shown in Fig. 2, a projection of $u_s(t,x)$, denoted as u_p, is either inside the feasible set or on the boundary of the feasible set depending on its magnitude. In either case, the projected control based on Sontag's formula guarantees stability even if there are input constraints. In Fig. 3, we can see that the control based on Sontag's formula cannot stay within the feasbile set even with some scaling due to its direction. In this case, a projection of $u_s(t,x)$ is not guaranteed to stay within the feasible set. However, it is straightforward to see that $\nu u_s(t,x)$, where $\nu > 1$, is still a stabilizing control in the case of $u \in I\!R^m$. As a result, for a stabilizing control $\nu u_s(t,x)$ with significantly large magnitude, the projection of $\nu u_s(t,x)$ to the rectangle area, denoted as u_p, is guaranteed to be on the boundary of the feasible set as shown in Fig. 3, which in turn guarantees stability. Note that the projection of the SDRE control (14) to the rectangle area is not guaranteed within the feasible set since the SDRE control does not guarantee global stability even in the case of unconstrained control inputs. That is, the SDRE control may not even point toward the unconstrained stabilizing area. Of course, this disadvantage can be corrected by projecting the SDRE control to the feasible set rather than the whole constrained input space at each time.

B. Saturation Tracking Controller Generated from the Feasible Set

Consider the following affine nonlinear time-varying system with control input u and exogenous input d

$$\dot{x} = f(t,x) + g(t,x)u + g_d(t,x)d, \tag{18}$$

where $x \in I\!R^n$, $u \in I\!R^m$, $d \in I\!R^r$, and $f : I\!R_+ \times I\!R^n \to I\!R^n$, $g : I\!R_+ \times I\!R^n \to I\!R^{n\times m}$, and $g : I\!R_+ \times I\!R^n \to I\!R^{n\times r}$ are locally Lipschitz in x and piecewise continuous in t.

We have the following definition for an input-to-state stabilizing control Lyapunov function (ISS-CLF) (see [25], [26], [24]).

Definition 1: A continuously differentiable function $V : I\!R_+ \times I\!R^n \to I\!R$ is an ISS-CLF for system (18) if it is positive-definite, decrescent, radially unbounded in x and there exist class $\mathcal{K}$ functions $\alpha(\cdot)$ and $\rho(\cdot)$ such that

$$\inf_{u\in I\!R^m} L_f V + L_g V u + L_{g_d} V d + \frac{\partial V}{\partial t} \le -\alpha(\|x\|), \quad \forall \|x\| \ge \rho(\|d\|).$$

Let $u = [v^c, \omega^c]^T$, Eq. (8) can be rewritten as

$$\dot{x} = f_2(t,x) + g_2(t,x)u, \tag{19}$$

where

$$f_2(t,x) = \begin{bmatrix} m\omega_r + \frac{1+x_2^2}{\pi_1^3} v_r \sin(x_0) + \frac{x_1 x_2}{\pi_1^3} v_r \cos(x_0) \\ v_r \sin\left(\frac{\bar{x}_0}{m}\right) \\ -v_r \cos(x_0) \end{bmatrix}$$

and

$$g_2(t,x) = \begin{bmatrix} -\frac{x_1 x_2}{\pi_1^3} & -(m - \frac{x_2}{\pi_1}) \\ 0 & x_2 \\ 1 & -x_1 \end{bmatrix}.$$

Given $W(x)$ in Eq. (9), where $x = [\bar{x}_0, x_1, x_2]^T$, we can always find a class $\mathcal{K}$ function α_w such that $\alpha_w(\|x\|) \le W(x)$, $\forall x$, following Lemma 3.5 in [25].

Lemma 2: Let $\mu = \sup_{\|x\|\to\infty} \alpha_w(\|x\|)$. If $\|L_{g_d} V d\| \le \sigma(\|d\|) < \theta\mu$, where $\sigma(\cdot)$ is a class $\mathcal{K}$ function and $0 < \theta < 1$, then $V(x)$ is also an ISS-CLF with input constraints (7) for system

$$\dot{x} = f_2(t,x) + g_2(t,x)u + g_d(t,x)d, \tag{20}$$

where $u = [v^c, \omega^c]$, d is the exogenous input, and $f_2(t,x)$ and $g_2(t,x)$ are given in Eq. (19).

Proof: It can be seen that

$$\begin{aligned} &\inf_{u\in\mathcal{U}_1} L_{f_2} V + L_{g_2} V u + L_{g_d} V d \\ &\le -W(x) + L_{g_d} V d \\ &\le -\alpha_w(\|x\|) + \|L_{g_d} V d\| \\ &\le -\alpha_w(\|x\|) + \sigma(\|d\|) \\ &\le -(1-\theta)\alpha_w(\|x\|) - \theta\alpha_w(\|x\|) + \sigma(\|d\|) \\ &\le -(1-\theta)\alpha_w(\|x\|), \quad \forall \|x\| \ge \alpha_w^{-1}\left(\frac{\sigma(\|d\|)}{\theta}\right) \end{aligned}$$

Note that $\alpha_w^{-1}(\cdot)$ in the last inequality is also a class $\mathcal{K}$ function of $\|d\|$ and is well defined since $\frac{\sigma(\|d\|)}{\theta} < \mu$. ■

Note that here $\alpha_w(\cdot)$ is a class $\mathcal{K}$ function instead of a class $\mathcal{K}_\infty$ function, which in turn imposes constraints for $\|d\|$. This can be explained from the constrained input perspective. In the case of $d = 0$, the derivative of the CLF cannot approach $-\infty$ as the tracking errors approach ∞ even with maximum control authority due to the saturated controls. As a result, $\alpha_w(\cdot)$ can only be a class $\mathcal{K}$ function in this case unlike the case when there are no input constraints.

Let

$$v^c = \begin{cases} v_{min}, & -\eta_v x_2 < \underline{v} \\ -\eta_v x_2, & \underline{v} \le -\eta_v x_2 \le \bar{v} \\ v_{max}, & -\eta_v x_2 > \bar{v} \end{cases}, \tag{21}$$

$$\omega^c = \begin{cases} \omega_{max}, & -\eta_\omega \bar{x}_0 < \underline{\omega} \\ -\eta_\omega \bar{x}_0, & \underline{\omega} \le -\eta_\omega \bar{x}_0 \le \bar{\omega} \\ -\omega_{max}, & -\eta_\omega \bar{x}_0 > \bar{\omega} \end{cases}. \tag{22}$$

In [14] we claimed that a variation of the the above control law globally asymptotically stabilizes system (19) with input constraints (3) for sufficiently large $\eta_v > 0$ and $\eta_\omega > 0$, which is made precise in Appendix VIII for review purpose since there is no explicit proof provided in [14].

It is obvious that the control law (21) and (22) rely on the state measurement x, y, and ψ. Due to measurement noise, there exist input uncertainties for system (19). We denote the actual control input to system (19) as $u = [v^c + \Delta v, \omega^c + \Delta\omega]^T$, where v^c and ω^c are given by Eqs. (21) and (22) and Δv and $\Delta\omega$ represent the uncertainties. Due to saturation constraints, we know that $|\Delta v| \leq v_{max} - v_{min}$ and $|\Delta\omega| \leq 2\omega_{max}$.

We have the following lemma considering input uncertainties.

Lemma 3: Let $b = [k_1 + \frac{1}{2}, m+1]^T$ and $\Delta u = [\Delta v, \Delta\omega]^T$. If $\|b\| \, \|\Delta u\| < \theta\mu$, where $0 < \theta < 1$, then $V(x)$ given by Eq. (10) is an ISS-Lyapunov function for system (20) with control input $u = [v^c, \omega^c]^T$ given by Eqs. (26) and (27), $g_d(t,x) = g_2(t,x)$, and $d = \Delta u$.

Proof: Noting that $\frac{\partial V}{\partial x} = [\frac{\bar{x}_0}{\pi_2}, k_1\frac{x_1}{\pi_1}, k_1\frac{x_2}{\pi_1}]$, we get that

$$L_{g_d}V = [-\frac{\bar{x}_0}{\pi_2}\frac{x_1 x_2}{\pi_1^3} + k_1\frac{x_2}{\pi_1}, -(m - \frac{x_2}{\pi_1})\frac{\bar{x}_0}{\pi_2}].$$

It can be verified that

$$\|L_{g_d}V\Delta u\| \leq \|L_{g_d}V\| \, \|\Delta u\| \leq \|b\| \, \|\Delta u\| \, ,$$

where the last inequality follows the fact that $\left|-\frac{\bar{x}_0}{\pi_2}\frac{x_1 x_2}{\pi_1^3} + k_1\frac{x_2}{\pi_1}\right| \leq k_1 + \frac{1}{2}$ and $\left|-(m - \frac{x_2}{\pi_1})\frac{\bar{x}_0}{\pi_2}\right| \leq m+1$. The result then directly follows Lemma 2. ■

V. Simulation Results

In this section, we simulate several scenarios where the four tracking controllers proposed in Section III and IV are applied to a small fixed-wing UAV to track a time-parameterized desired trajectory that satisfies the constraints (4).

The parameters used in the simulation are chosen as $\alpha_\psi = 5$, $\alpha_v = 50$, $\epsilon_v = 0.2$ (m/s), $\epsilon_\omega = 0.2$ (rad/s), $k_1 = 2$, $\gamma_0 = \gamma_1 = \gamma_2 = 0.5$, $\eta_\omega = \eta_v = 10$, and $m = 1$. Note that the value for m is much lower than the theoretical lower bound defined in [14]. However, as we will see in the following, the controllers work well using this value, which implies the robustness of the controllers to parameter variations. We assume arbitrarily that the commanded velocity and heading rate are saturated at $v^c \in [1.0, 1.8]$ (m/s) and $|\omega^c| \leq 1.5$ (rad/s) to test the performance of the controllers.

Fig. 4 shows the desired trajectory generated from the DTS and the actual trajectories generated from the four tracking controllers under small initial errors. For the SDRE controller, the weighting matrices are chosen as $Q(x) = \mathrm{diag}([1,1,1])$ and $R(x) = \frac{100}{(\sqrt{x_0^2+x_1^2+x_2^2+0.2})}\mathrm{diag}([1,1])$. Fig. 5 shows the distance and heading tracking errors and Fig. 6 shows the desired and actual control inputs under the same initial conditions. We can see that all four controllers guarantee asymptotic tracking. Although the controller based on Sontag's formula does not explicitly consider the input constraints, the tracking errors using the projection of that controller converge fastest. On the other hand, the controller based on the geometric approach converge slowest, which is due to the slow convergence of the heading in this case. In addition, both the control inputs based on Sontag's formula and the geometric approach have chattering phenomenon compared to the SDRE and saturation controllers. This can be explained from the perspective that the desired heading rate is highly switching and discontinuous (piecewise continuous in this case) and the original Sontag's formula is designed for smooth functions and has no saturation considerations. As a comparison, saturation controller is designed with respect to the properties of the original system and accouts for the input constraints explicitly. The SDRE controller can also achieve good performance even if there is no explicit consideration for input constraints in the controller design.

Fig. 7 and 8 show the desired actual trajectories and the tracking errors respectively under large initial errors. The weighting matrices for the SDRE controller are chosen the same as the small inital errors case. It can be seen that the saturation controller and the controller based on the geometric approach are superior to the other two by explicitly accounting for the input constraints during the controller design procedure. In fact, the SDRE controller has the worst performance for heading tracking due to heading rate saturation.

Fig. 9 and 10 show a comparison between the SDRE controller and the saturation controller under small and large initial errors respectively. Here the weighting matrices for the SDRE controller is chosen as $Q(x) = \mathrm{diag}([1,1,1])$ and $R(x) = \mathrm{diag}([8,10])$. We can see that by properly choosing the weighting matrices $Q(x)$ and $R(x)$, the SDRE controller can achieve better performance than the saturation controller under small initial errors in Fig. 9, which can be expected since the SDRE controller is proved to be locally asymptotically stable and suboptimal. However, using the same weighting matrices but under large initial errors , the SDRE controller achieves much worse performance than the saturation controller as shown in Fig. 10 due to the input constraints.

Fig. 11 and 12 show the performance of the SDRE controller without and with input constraints respectively, where $Q(x) = \mathrm{diag}([1,1,1])$ and $R(x) = \mathrm{diag}([0.1, 0.01])$. We can see that the SDRE controller becomes unstable with these inapproapiate weighting matrices as shown in Fig. 11. Even if good tracking performance can be achieved without input constraints in Fig. 12, huge control efforts are needed in this case.

Fig. 13 shows the tracking errors of the four controllers with measurement noise. Here we assume that there are zero mean and unit variance white nosie associated with the position measurement and zero mean and 15 degree variance white noise associated with the heading measurement. The weighting matrices for the SDRE controller are chosen the same as those in Fig. 9 and 10. We can see that the saturation controller has the smallest steady-state tracking errors. Under the same settings, the SDRE controller is no longer superior to the saturation controller subject to measurement noise compared to Fig. 9.

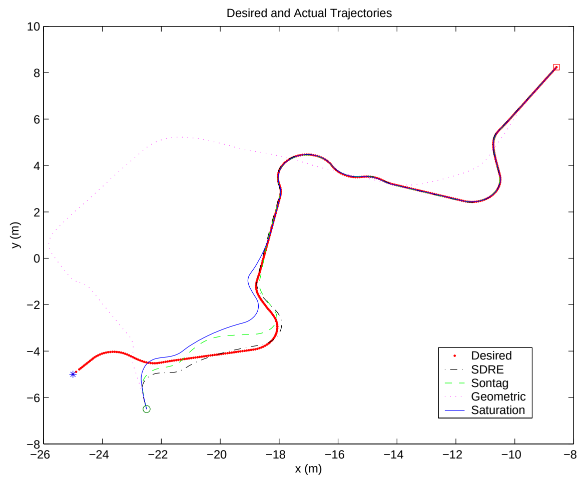

Fig. 4. The desired and actual trajectories under small initial errors.

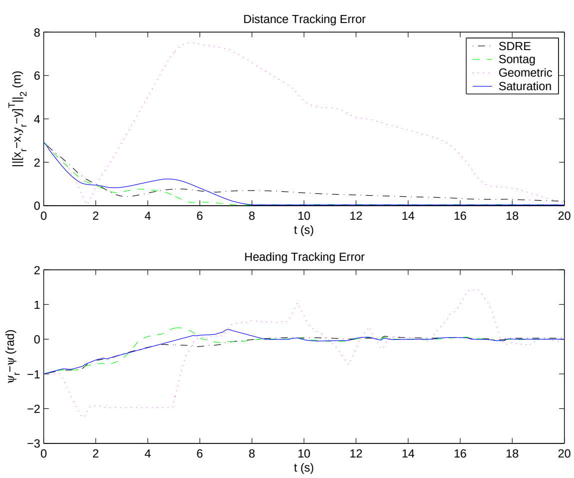

Fig. 5. The trajectory tracking errors under small initial errors.

VI. Conclusion

Constrained nonlinear tracking control for unmanned air vehicles is studied. Non-CLF based control approach and constrained CLF based control approaches are derived to achieve asymptotically tracking. Input uncertainties are also addressed using input-to-state stability. Detailed simulation results showed the advantage and disadvantage of each approach under different situations.

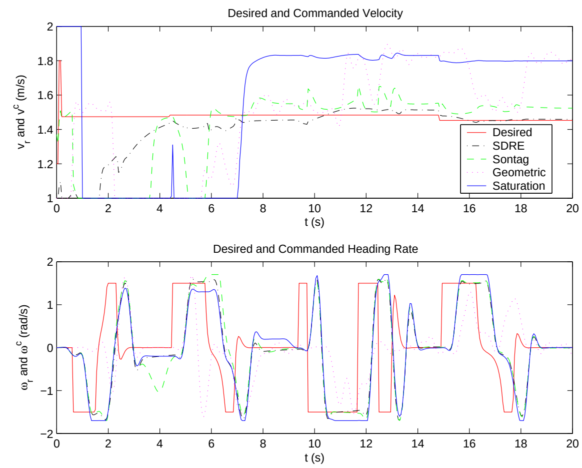

Fig. 6. The desired and actual control inputs under small initial errors.

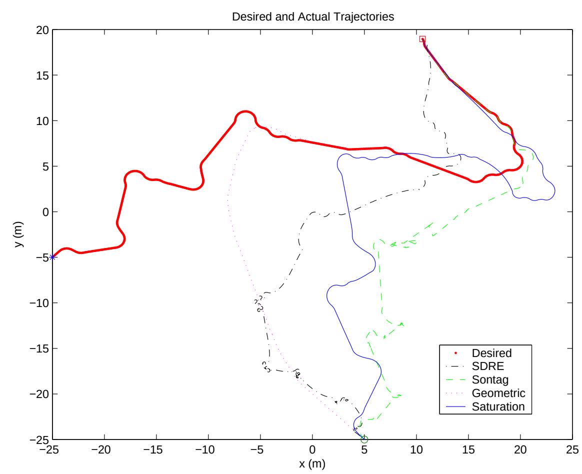

Fig. 7. The desired and actual trajectories under large initial errors.

VII. Acknowledgments

This work was funded by AFOSR grants F49620-01-1-0091 and F49620-02-C-0094, and by DARPA grant NBCH1020013.

VIII. Appendix

Define

$$M_3 \triangleq \max\{0, \sup_{\substack{0<|\alpha|<1\\|\beta|<1\\0<c\leq 1}} (\alpha^2+1)\frac{\rho_1}{\alpha^2}\} \tag{23}$$

$$M_4 \triangleq \max\{0, \sup_{\substack{0<\alpha<1\\|\beta|<1}} (\alpha^2+1)\frac{\rho_2}{\alpha^2}\} \tag{24}$$

$$M_5 \triangleq \max\{0, \sup_{0<|\alpha|<1} (\alpha^2+1)\frac{\rho_3}{\alpha^2}\}, \tag{25}$$

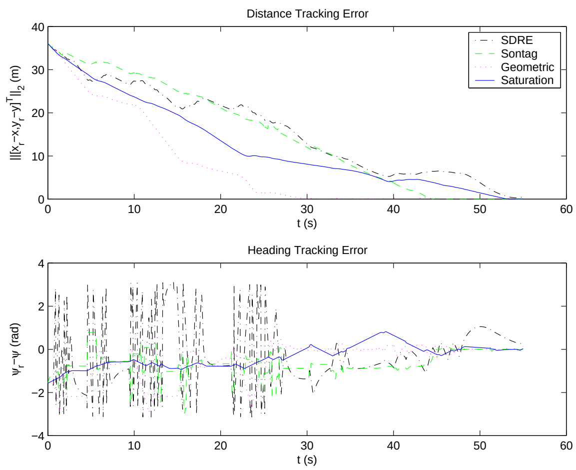

Fig. 8. The trajectory tracking errors under larege initial errors..

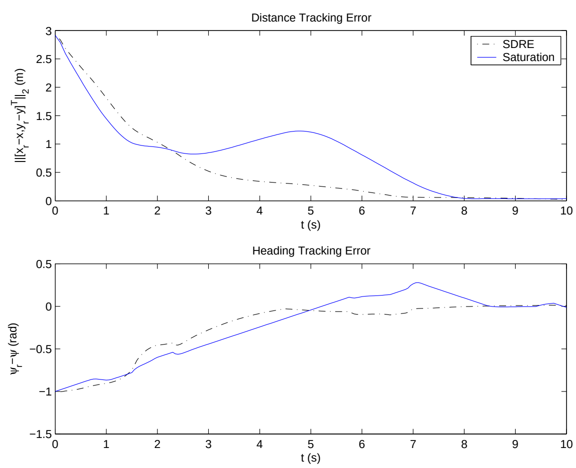

Fig. 9. The comparison between SDRE controller and saturation controller under small initial errors.

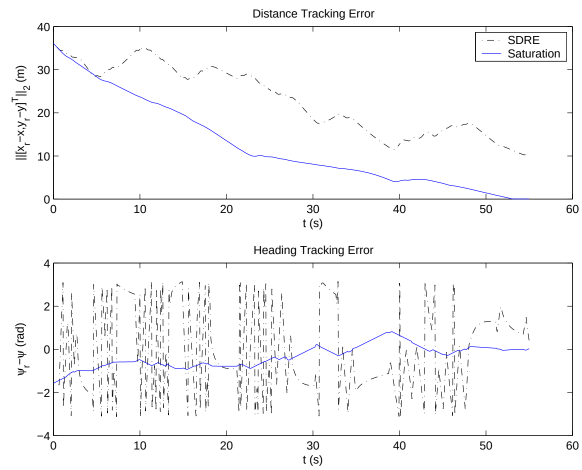

Fig. 10. The comparison between SDRE controller and saturation controller under large initial errors.

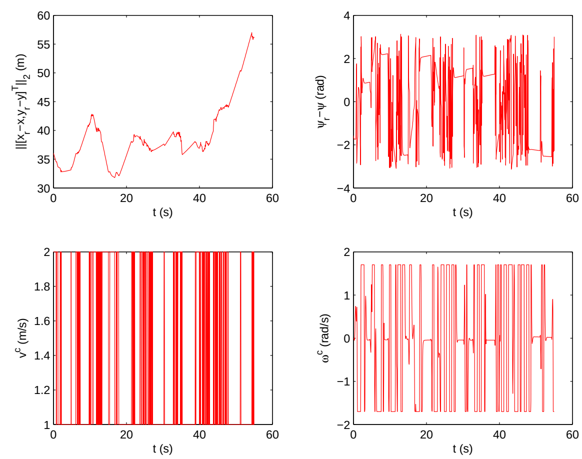

Fig. 11. The performance of SDRE controller using inappropriate weighting matrices with input constraints.

where

$$
\begin{aligned}
\rho_1 &= \left(k_1\beta + \frac{\alpha}{\sqrt{\alpha^2+1}}c\right)\sin\left(\frac{\alpha-\beta}{m}\right) \\
&\quad + k_1\gamma_1\beta\sin\left(\frac{\beta}{m}\right) \\
\rho_2 &= \frac{|\alpha|}{\sqrt{\alpha^2+1}}(\omega_{max}-\epsilon_\omega) \\
&\quad + (k_1-\frac{1}{2})\left[v_{min}-(v_{min}+\epsilon_v)\cos\left(\frac{\alpha-\beta}{m}\right)\right] \\
&\quad + \gamma_2(k_1-\frac{1}{2})\left[(v_{min}+\epsilon_v)\cos\left(\frac{\beta}{m}\right)-v_{min}\right] \\
\rho_3 &= \frac{|\alpha|}{\sqrt{\alpha^2+1}}(\omega_{max}-\epsilon_\omega)+(k_1-\frac{1}{2})(\gamma_2-1)\epsilon_v,
\end{aligned}
$$

and k_1, γ_1, γ_2, and m are defined in Section II.

It is easy to see that M_3, M_4, and M_5 in Eqs. (23), (24), and (25) are bounded as $|\alpha|$ approaches 1. Note that $1 < (\alpha^2+1) < 2$ since $0 < |\alpha| < 1$. For Eq. (23), two cases will be considered with regard to β. In the case of $\beta = 0$, $(\alpha^2+1)\rho_1/\alpha^2 = (\sqrt{\alpha^2+1})c\sin(\frac{\alpha}{m})/\alpha$, which is bounded by $1/m$ as α approaches 0. In the case of $\beta \neq 0$, as $|\alpha|$ approaches 0, ρ_1 approaches $k_1(\gamma_1-1)\beta\sin(\frac{\beta}{m})$, which is negative since $0 < \gamma_1 < 1$ and $\left|\frac{\beta}{m}\right| < \frac{1}{m} < \frac{\pi}{4}$ following $m > \kappa$ [14]. Thus $M_3 = 1/m$ as $|\alpha|$ approaches 0. For Eq. (24), as $|\alpha|$ approaches 0, ρ_2 approaches $(k_1-1/2)(\gamma_2-1)[(v_{min}+\epsilon_v)\cos\left(\frac{\beta}{m}\right)-v_{min}]$, which is also negative following $m > \kappa$ [14]. Thus $M_4 = 0$ as $|\alpha|$ approaches 0. For Eq. (25), as $|\alpha|$ approaches 0, ρ_3 approaches $(k_1-\frac{1}{2})(\gamma_2-1)\epsilon_v$, which is also negative. Thus $M_5 = 0$ as $|\alpha|$ approaches 0. Therefore M_3, M_4, and M_5 are finite and can be found by straightforward numerical techniques.

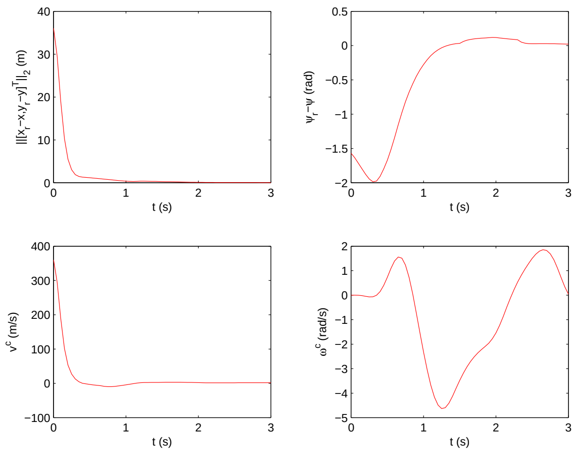

Fig. 12. The performance of SDRE controller using inappropriate weighting matrices without input constraints.

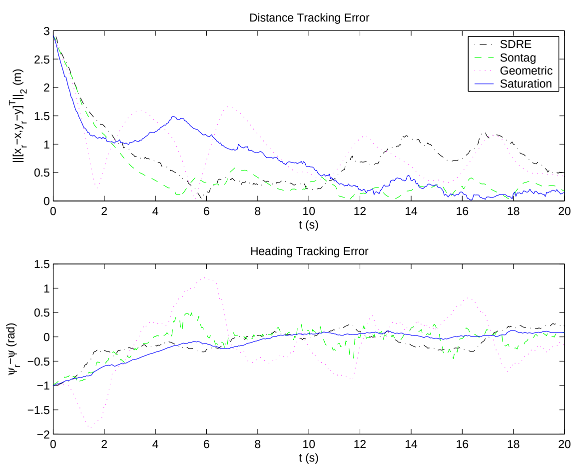

Fig. 13. The trajectory tracking errors under measurement noise.

Lemma 4: If

$$v^c = \begin{cases} v_{min}, & -\eta_v x_2 < \underline{v} \\ -\eta_v x_2, & \underline{v} \le -\eta_v x_2 \le \bar{v} \\ v_{max}, & -\eta_v x_2 > \bar{v} \end{cases}, \tag{26}$$

$$\omega^c = \begin{cases} \omega_{max}, & -\eta_\omega \bar{x}_0 < \underline{\omega} \\ -\eta_\omega \bar{x}_0, & \underline{\omega} \le -\eta_\omega \bar{x}_0 \le \bar{\omega} \\ -\omega_{max}, & -\eta_\omega \bar{x}_0 > \bar{\omega} \end{cases}, \tag{27}$$

and

$$\eta_\omega > \max\{\epsilon_\omega, \frac{d_3}{m-1}, \frac{d_4}{m-1}\} \tag{28}$$

$$\eta_v > \frac{\omega_{max} - \epsilon_\omega}{2k_1 - 1} + \gamma_2 \epsilon_v, \tag{29}$$

where

$$d_3 = M_3(v_{max} - \epsilon_v) + \gamma_0 + \frac{1}{2}(\omega_{max} - \epsilon_\omega)$$
$$d_4 = M_3(v_{max} - \epsilon_v) + \gamma_0 + \max\{M_4, M_5\},$$

then $u = [v^c, \omega^c]^T$ globally asymptotically stabilizes system (19).

Proof: To show that $u = [v^c, \omega^c]^T$ globally asymptotically stabilizes system (19), it is equivalent to show that $k_{sat}(t,x) = [u_0, u_1]$ globally asymptotically stabilizes system (16), where

$$u_0 = \begin{cases} \underline{\omega}, & -\eta_\omega \bar{x}_0 < \underline{\omega} \\ -\eta_\omega \bar{x}_0, & \underline{\omega} \le -\eta_\omega \bar{x}_0 \le \bar{\omega} \\ \bar{\omega}, & -\eta_\omega \bar{x}_0 > \bar{\omega} \end{cases} \tag{30}$$

$$u_1 = \begin{cases} \underline{v}, & -\eta_v x_2 < \underline{v} \\ -\eta_v x_2, & \underline{v} \le -\eta_v x_2 \le \bar{v} \\ \bar{v}, & -\eta_v x_2 > \bar{v} \end{cases}. \tag{31}$$

Obviously $k_{sat}(t,x)$ is locally Lipschitz in x and piecewise continuous in t. We will show that $\dot{V} = L_{f_1}V + L_{g_1}Vk_{sat}(t,x) \le -W(x)$.

Note that

$$\dot{V} + W(x) = \delta_1 + \delta_2 + \delta_3 + \delta_4, \tag{32}$$

where

$$\delta_1 = \sigma_3 + \frac{\bar{x}_0}{\pi_2}\frac{1+x_2^2}{\pi_1^3} v_r \sin\left(\frac{\bar{x}_0}{m} - \frac{x_1}{m\pi_1}\right)$$
$$\delta_2 = \frac{\bar{x}_0}{\pi_2}\left(m - \frac{x_2}{\pi_1}\right) u_0 + \gamma_0 \left(\frac{\bar{x}_0}{\pi_2}\right)^2$$
$$\delta_3 = \frac{\bar{x}_0}{\pi_2}\frac{x_2}{\pi_1}\omega_r$$
$$\delta_4 = \sigma_1 u_1 + \sigma_2,$$

where

$$\sigma_1 = \left(k_1 - \frac{\bar{x}_0 x_1}{\pi_2 \pi_1^2}\right)\left(\frac{x_2}{\pi_1}\right)$$
$$\sigma_2 = \gamma_2(k_1 - \frac{1}{2})\left(\frac{x_2}{\pi_1}\right)^2 \left[(v_{\min} + \epsilon_v)\cos\left(\frac{x_1}{m\pi_1}\right) - v_{\min}\right]$$
$$\sigma_3 = k_1\left(\frac{x_1}{\pi_1}\right)\left[v_r \sin(\frac{\bar{x}_0}{m} - \frac{x_1}{m\pi_1}) + \gamma_1(v_{\min} + \epsilon_v)\sin\left(\frac{x_1}{m\pi_1}\right)\right].$$

Four cases will be considered as follows.

Case 1: $-\eta_\omega \bar{x}_0 \notin [\underline{\omega}, \bar{\omega}]$ **and** $-\eta_v x_2 \notin [\underline{v}, \bar{v}]$**.**
In this case, the saturation functions are the same as the discontinuous signum like functions used to prove that V is a CLF in [14], which implies that $\dot{V} \le -W(x)$ in this case.
Case 2: $-\eta_\omega \bar{x}_0 \in [\underline{\omega}, \bar{\omega}]$ **and** $-\eta_v x_2 \in [\underline{v}, \bar{v}]$**.**
In this case, we can see that $u_0 = -\eta_\omega \bar{x}_0$ and $u_1 = -\eta_v x_2$. We also know that $|\bar{x}_0| < 1$ since $\eta_\omega > \epsilon_\omega$.

Noting that

$$\delta_1 \leq M_3(v_{max} - \epsilon_v)\left(\frac{\bar{x}_0}{\pi_2}\right)^2 \quad (33)$$

$$\delta_2 \leq [-(m-1)\eta_\omega + \gamma_0]\left(\frac{\bar{x}_0}{\pi_2}\right)^2 \quad (34)$$

$$\delta_3 \leq \frac{1}{2}\left[\left(\frac{\bar{x}_0}{\pi_2}\right)^2 + \left(\frac{x_2}{\pi_1}\right)^2\right](\omega_{max} - \epsilon_\omega) \quad (35)$$

$$\delta_4 \leq (k_1 - \frac{1}{2})(\gamma_2\epsilon_v - \eta_v)\left(\frac{x_2}{\pi_1}\right)^2, \quad (36)$$

where Eq. (33) comes from Eq. (23) by letting $\alpha = \bar{x}_0$, $\beta = x_1/\pi_1$, and $c = (1 + x_2^2)/\pi_1^3$, and Eq. (35) follows Young's Inequality. Therefore,

$$\dot{V} + W(x) \leq [d_3 - (m-1)\eta_\omega]\left(\frac{\bar{x}_0}{\pi_2}\right)^2 + \left[\frac{1}{2}(\omega_{max} - \epsilon_\omega) + (k_1 - \frac{1}{2})(\gamma_2\epsilon_v - \eta_v)\right]\left(\frac{x_2}{\pi_1}\right)^2,$$

which is nonpositive since $\eta_\omega > d_3/(m-1)$ and $\eta_v > \frac{\omega_{max} - \epsilon_\omega}{2k_1 - 1} + \gamma_2\epsilon_v$.

Case 3: $-\eta_\omega\bar{x}_0 \in [\underline{\omega}, \bar{\omega}]$ **and** $-\eta_v x_2 \notin [\underline{v}, \bar{v}]$.

In this case, $|\bar{x}_0| < 1$, δ_1 and δ_2 follow the same inequalities (33) and (34), and $\delta_3 \leq \left(\frac{|x_2|}{\pi_1}\right)\left(\frac{|\bar{x}_0|}{\pi_2}\right)(\omega_{max} - \epsilon_\omega)$. Note that $\underline{v} < 0$ from $m > \kappa$ [14] and $\bar{v} \leq \epsilon_v$. If $-\eta_v x_2 < \underline{v}$, we can get that $x_2 > -\frac{\underline{v}}{\eta_v} > 0$. Thus $(\delta_3 + \delta_4) \leq \left(\frac{|x_2|}{\pi_1}\right) M_4 \left(\frac{\bar{x}_0}{\pi_2}\right)^2 \leq M_4\left(\frac{\bar{x}_0}{\pi_2}\right)^2$. If $-\eta_v x_2 > \bar{v}$, we can get that $x_2 < -\frac{\bar{v}}{\eta_v} < 0$. Thus $(\delta_3 + \delta_4) \leq \left|\frac{x_2}{\pi_1}\right| M_5 \left(\frac{\bar{x}_0}{\pi_2}\right)^2 \leq M_5\left(\frac{\bar{x}_0}{\pi_2}\right)^2$. Therefore, $\dot{V} + W(x) \leq 0$ since $\eta_\omega > d_4/(m-1)$.

Case 4: $-\eta_\omega\bar{x}_0 \notin [\underline{\omega}, \bar{\omega}]$ **and** $-\eta_v x_2 \in [\underline{v}, \bar{v}]$.

In this case, $u_0 \mathrm{sign}(\bar{x}_0) \leq -\epsilon_\omega$ and δ_4 follows the same inequality (36). It can be seen that $(\sigma_1 u_1 + \sigma_2) \triangleq \delta_4 \leq 0$ since $\eta_v > \gamma_2\epsilon_v$. We can see that $\dot{V} + W(x) \leq -\epsilon_\omega \frac{|\bar{x}_0|}{\pi_2}(m - \frac{x_2}{\pi_1}) + \sigma_3 + \sigma_4$. Then following the proof that V is a CLF in [14], we know that $\dot{V} + W(x) \leq 0$ is guaranteed based on the choice of m.

Combining these four cases gives the desired result. ■

IX. REFERENCES

[1] A. Stoorvogel and A. Saberi, "Special issue on control of systems with bounded control," *International Journal of Robust and Nonlinear Control*, vol. 9, 1999.

[2] D. S. Bernstein and A. N. Michel, "A chronological bibliography on saturating actuators," *International Journal of Robust and Nonlinear Control*, vol. 5, pp. 375–380, 1995.

[3] E. D. Sontag, "A Lyapunov-like characterization of asymptotic controllability," *SIAM Journal on Control and Optimization*, vol. 21, pp. 462–471, May 1983.

[4] Z. Artstein, "Stabilization with relaxed controls," *Nonlinear Analysis, Theory, Methods, and Applications*, vol. 7, no. 11, pp. 1163–1173, 1983.

[5] D. Q. Mayne and H. Michalska, "Receding horizon control of nonlinear systems," *IEEE Transactions on Automatic Control*, vol. 35, no. 7, pp. 814–824, 1990.

[6] E. F. Camacho and C. Bordons, *Model Predictive Control*. Springer Verlag, 1999.

[7] B. Kouvaritakis and M. Cannon, *Nonlinear Predictive Control Theory and Practice*. London, United Kingdom: The Institution of Electrical Engineers, 2001.

[8] Y. Lin and E. Sontag, "Control-Lyapunov universal formulas for restricted inputs," *Control-Theory and Advanced Technology*, vol. 10, pp. 1981–2004, December 1995.

[9] Y. Lin and E. D. Sontag, "Universal formula for stabilization with bounded controls," *Systems and Control Letters*, vol. 16, pp. 393–397, June 1991.

[10] J. A. Primbs, V. Nevistić, and J. C. Doyle, "Nonlinear optimal control: A control Lyapunov function and receding horizon perspective," *Asian Journal of Control*, vol. 1, no. 1, pp. 14–24, 1999.

[11] M. Sznaier and R. Suárez, "Suboptimal control of constrained nonlinear systems via receding horizon state dependent riccati equations," in *Proceedings of the IEEE Conference on Decision and Control*, pp. 3832–3837, 2001.

[12] Z.-P. Jiang, E. Lefeber, and H. Nijmeijer, "Saturated stabilization and track control of a nonholonomic mobile robot," *Systems and Control Letters*, vol. 42, pp. 327–332, 2001.

[13] T.-C. Lee, K.-T. Song, C.-H. Lee, and C.-C. Teng, "Tracking control of unicycle-modeled mobile robots using a saturation feedback controller," *IEEE Transactions on Control Systems Technology*, vol. 9, pp. 305–318, March 2001.

[14] W. Ren and R. W. Beard, "Clf-based tracking control for uav kinematic models with saturation constraints," in *Proceedings of the IEEE Conference on Decision and Control*, (Maui, Hawaii), December 2003. (to appear).

[15] J. R. Cloutier, C. N. D'Souza, and C. P. Mracek, "Nonlinear regulation and nonlinear H_∞ control via the state-dependent Riccati equation technique," in *IFAC World Congress*, (San Francisco, California), 1996.

[16] J. R. Cloutier, "State-dependent riccati equation techniques: An overview," in *Proceedings of the American Control Conference*, pp. 932–936, 1997.

[17] E. Sontag and Y. Wang, "New characterizations of input-to-state stability," *IEEE Transactions on Automatic Control*, vol. 41, pp. 1283–1294, September 1996.

[18] J. W. Curtis and R. W. Beard, "Satisficing: A new approach to constructive nonlinear control," *IEEE Transactions on Automatic Control*, (in review).

[19] D. Kingston, R. Beard, T. McLain, M. Larsen, and

W. Ren, “Autonomous vehicle technologies for small fixed wing uavs,” in *AIAA 2nd Unmanned Unlimited Systems, Technologies, and Operations–Aerospace, Land, and Sea Conference and Workshop & Exhibit*, (San Diego, CA), September 2003. Paper no. AIAA-2003-6559.

[20] A. W. Proud, M. Pachter, and J. J. D'Azzo, “Close formation flight control,” in *Proceedings of the AIAA Guidance, Navigation, and Control Conference*, (Portland, OR), pp. 1231–1246, August 1999. Paper No. AIAA-99-4207.

[21] R. W. Beard, T. W. McLain, M. Goodrich, and E. P. Anderson, “Coordinated target assignment and intercept for unmanned air vehicles,” *IEEE Transactions on Robotics and Automation*, vol. 18, no. 6, pp. 911–922, 2002.

[22] P. Dorato, C. Abdallah, and V. Cerone, *Linear-Quadratic Control: An Introduction*. Englewood Cliffs, New Jersey: Prentice Hall, 1983.

[23] E. D. Sontag, “A ‘universal’ construction of Artstein's theorem on nonlinear stabilization,” *System & Control Letters*, vol. 13, pp. 117–123, 1989.

[24] M. Krstić and H. Deng, *Stabilization of Nonlinear Uncertain Systems*. Communication and Control Engineering, London: Springer, 1998.

[25] H. K. Khalil, *Nonlinear Systems*. Upper Saddle River, NJ: Prentice Hall, 2nd ed., 1996.

[26] A. Isidori, *Nonlinear Control Systems II*. Communication and Control Engineering, New York, New York: Springer Verlag, 1999.